TCCI: Taming Co-Channel Interference for Wireless LANs

Adnan Quadri, Hossein Pirayesh, Pedram Kheirkhah Sangdeh, and Huacheng Zeng {adnan.quadri,hossein.pirayesh,pedram.kheirkhahsangdeh,huacheng.zeng}@louisville.edu
Department of Electrical and Computer Engineering, University of Louisville, Louisville, KY 40292

ABSTRACT

Co-channel interference is a fundamental issue in WLANs. Although many results have been developed to handle co-channel interference for concurrent transmission, most of them require network-wide fine-grained synchronization and data sharing among access points (APs). Such luxuries, however, are not affordable in many WLANs due to their hardware limitation and data privacy concern. In this paper, we present TCCI, a co-channel interference management scheme to enable concurrent transmission in WLANs. TCCI requires neither network-wide fine-grained synchronization nor inter-network data sharing, and therefore is amenable to realworld implementation. The enabler of TCCI is a new detection and beamforming method for an AP, which is capable of taming unknown interference by leveraging its multiple antennas. We have built a prototype of TCCI on a wireless testbed and demonstrated its compatibility with commercial Atheros 802.11 devices. Experiments show that TCCI allows co-located APs to serve their users simultaneously and achieves significant throughput gain (up to 113%) compared to the existing interference-avoidance scheme.

1 INTRODUCTION

Wireless spectrum is limited. We may have experienced the failure of Internet connection in busy Wi-Fi networks such as conference rooms, apartments and university dormitories. Such failure is not caused by the lack of advances in wireless devices. In fact, wireless devices such as access points (APs) and various user devices (a.k.a. stations or STAs) have improved remarkably in the past decades through innovations such as powerful computation capability and multi-antenna technology. The failure of Wi-Fi connections is actually caused by co-channel interference. The reality is, after three decades of evolution, most Wi-Fi networks are still limited to the interference avoidance paradigm, which allows only one of many co-located APs to access the spectrum at a time. Consequently, the performance of whole network is throttled by that particular AP, while other APs are forced to remain idle.

Recently, sophisticated techniques have been proposed to handle the co-channel interference in WLANs [20]. These techniques are under different names, such as network MIMO [15, 34] and joint multi-user processing [5, 35]. The basic idea of these techniques is to jointly process the signals at all APs so that all the antennas on the APs can be fully utilized for multi-user MIMO transmission. By doing so, all the APs can be regarded as a unified giant AP. While these interference management techniques offer significant throughput gain, they require network-wide fine-grained synchronization and data sharing among the APs. These requirements, however, are not achievable in some WLANs. We explain the two reasons as follows. *i) Network-wide fine-grained synchronization:* To achieve joint signal processing for network MIMO, it requires inter-AP synchronization for downlink transmission and inter-STA synchronization for uplink transmission [2]. The time misalignment should be less than

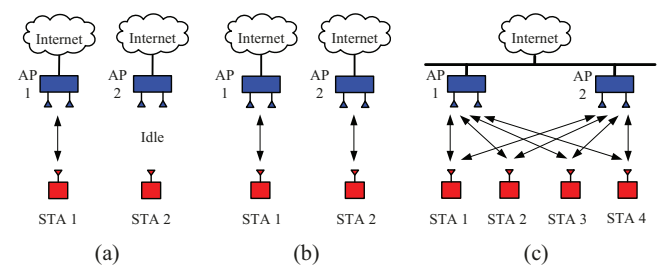


Figure 1: TCCI versus existing techniques. Interference is not shown in the figures. (a) Interference avoidance: Only one packet can be sent in a time instance. (b) TCCI: Two packets can be sent simultaneously in the absence of network-wide fine-grained synchronization and inter-AP data sharing. (c) Network MIMO: Four packets can be sent simultaneously, but it requires network-wide fine-grained synchronization and inter-AP data sharing, which are not achievable in WLANs.

the cyclic prefix (CP) of an OFDM symbol (800 ns in IEEE 802.11ac [18]). However, many WLANs cannot afford such fine-grained time synchronization due to the device hardware limitation [26]. For example, when multiple STAs send their packets to the APs, these packets do not arrive at the APs at the same time. The time misalignment of the packets is caused by various delays, including the detection delay of the announcement packet, the hardware Tx/Rx turnaround delay, and the propagation delay. Typically, the time misalignment of the packets is larger than the OFDM CP duration and, as a result, the APs cannot decode the misaligned packets. Due to the time synchronization issue, IEEE 802.11ac [18] specifies very loose bounds on hardware turnaround time (10 µs), and uplink MU-MIMO was discussed in 802.11ac Work Groups but eventually not included in 802.11ac. ii) Data sharing among the APs: Data sharing is not permitted in the WLANs where different APs belong to different owners who have concern about their data privacy. One may argue that the data traffic can be protected by data encryption. That is true in real WLANs, but the encrypted traffic also suffers from privacy leakage. The privacy of encrypted data traffic could be compromised by advanced traffic analysis techniques [39]. Therefore, the users may be reluctant to expose their data traffic to other people. In light of these two issues, we intend to enable concurrent transmission for the co-located WLANs in the absence of network-wide fine-grained synchronization and inter-network

In this paper, we present TCCI, a co-channel interference management scheme to enable simultaneous transmission for co-located WLANs. The basic idea of TCCI is that each WLAN works independently for signal processing and its AP mitigates the inter-network co-channel interference in the spatial domain by leveraging its multiple antennas. Different from network MIMO, TCCI requires neither inter-network fine-grained synchronization nor inter-network

data sharing, and therefore is amenable to practical implementation. Figure 1 illustrates the difference between TCCI and two existing techniques. Compared to the interference avoidance technique (e.g., CSMA and TDMA), TCCI enables two co-located WLANs to access the spectrum simultaneously, provided that both APs have two antennas. Although network MIMO can serve more users than TCCI, it requires inter-network fine-grained synchronization and data sharing, which are not achievable in many real-world WLANs.

The motivation behind TCCI is that an AP (Wi-Fi routers) typically has more antennas than an STA. For example, a WiFi router is very common to have six antennas, but an STA (e.g., smartphone, laptop, and IoT device) typically has one or two antennas due to its physical-size and power constraints. TCCI exploits the AP' extra antennas to mitigate the co-channel interference. The main challenge in the co-channel interference mitigation is the lack of fine-grained synchronization among the network devices. To address this challenge, TCCI assumes no knowledge about interference and designs a spatial filter to mitigate unknown interference. Specifically, in the uplink, each AP receives the desired signal from its serving STA and the interfering signal from its unintended STAs. To decode its desired signals, the AP employs a linear spatial filter for co-channel interference cancellation and channel equalization on each OFDM subcarrier. A natural question is how to design the spatial filter without channel knowledge. In TCCI, the spatial filter is constructed using the interfered reference symbols embedded into the desired signals. Surprisingly, such an approach yields a superior performance in the signal detection. In the downlink, instead of constructing the beamforming filters based on channel knowledge, TCCI uses the decoding filters obtained by an AP in the uplink as its beamforming filters. This beamforming design is reliant on channel reciprocity, which we can be achieved through relative channel calibration at the APs. Collectively, TCCI manages to enable concurrent transmission in the absence of inter-network fine-grained synchronization and inter-network data sharing.

We have built a prototype of TCCI on a wireless testbed consisting of USRP devices and commercial off-the-shelf (COTS) Qualcomm Atheros 802.11 dongles. TCCI have successfully demonstrated its compatibility with COTS Atheros 802.11 client devices. With a modified Linux driver for Atheros 802.11 dongles, TCCI enables our custom-designed APs to serve their respective Atheros 802.11 dongles simultaneously in the absence of inter-user synchronization and data exchange. More specifically, our experimental results of TCCI show that (i) two APs with each having two antennas can serve two STAs simultaneously; (ii) three APs with each having three antennas can serve three STAs simultaneously; and (iii) two APs with each having four antennas can serve four STAs simultaneously. Moreover, TCCI offers significant throughput gain compared to the TDMA-based interference avoidance approach. The throughput gains are 77%, 113%, and 50% for the above three networks.

2 PROBLEM DESCRIPTION

We consider a set of co-located WLANs (e.g., in university dormitory or compact apartment complex) as shown in Figure 2, each of which consists of an AP and their serving STAs. For ease of explanation, we consider the case where each AP has one active STA in service and

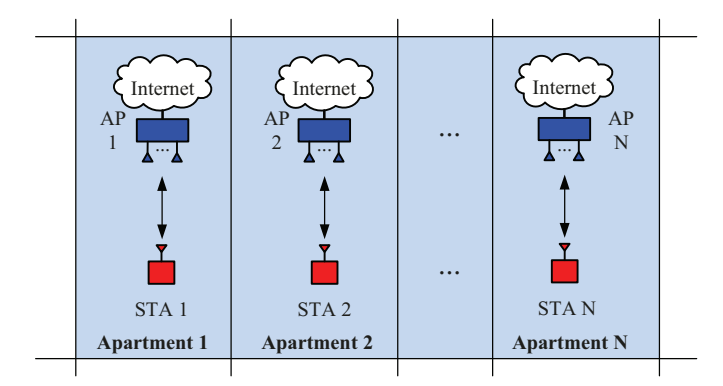


Figure 2: Concurrent data communications in N WLANs. Cochannel interference between WLANs is not shown in the figure.

each STA has one antenna. In the end, we shall see that TCCI works in the generic case where the APs have heterogeneous antenna configuration, the APs serve more than one STA, or the STAs have multiple antennas. For this set of WLANs, we have the following three assumptions.

First, we assume that the APs use the same spectrum band for the communications between themselves and their serving STAs. The APs do not have the permission to share their users' data for privacy reason. They cannot share the estimated channel state information (CSI) with each other, either. The STAs are commodity Wi-Fi client devices, which cannot achieve sub-microsecond time synchronization in practice.

Second, we assume that the number of AP's antennas is greater than or equal to the number of active STAs, i.e., $M \ge N$, where M is the number of an AP's antennas and N is the number of APs (also the number of STAs). We note that it is not fair to compare TCCI with network MIMO, which does not require this assumption ($M \ge N$). This is because network MIMO is not feasible in these WLANs due to the absence of network-wide fine-grained synchronization and data sharing among the APs.

Third, we assume that $N \leq M \leq 8$. The assumption is made based on the observation that the maximum number of antennas on an existing WiFi router is eight. Meanwhile, it is noteworthy that our intention is not to design a concurrent transmission scheme that scales with the number of APs. Instead, we intend to design a scheme that works in practical network settings (e.g., $N \leq M \leq 8$). **Our Objective and Design Challenge:** When the WLANs work in the TDMA mode, only one WLAN can access the spectrum in a time period and other WLANs will be forced to be idle. Our objective is to enable concurrent transmission among the WLANs, with respect to the fact that the network-wide fine-grained synchronization and data sharing among the APs are not achievable for network MIMO. Towards this objective, we propose TCCI to tame the co-channel interference by leveraging the multiple antennas on the APs.

The main challenge lies in the co-channel interference management in the absence of network-wide fine-grained time synchronization. TCCI addresses this challenge by developing a new signal detection method that does not require channel knowledge, while being capable of decoding the signal in the presence of unknown

interference. Based on this signal detection method, TCCI assembles a holistic scheme to enable concurrent transmission in both uplink and downlink of co-located WLANs.

3 UPLINK SIGNAL DETECTION IN THE FACE OF UNKNOWN INTERFERENCE

In this section, we consider the concurrent uplink transmission from the N STAs to the N APs in Figure 2. For each AP, we intend to design a signal detection method that can decode its desired signal in the face of co-channel interference. As we explained before, the STAs in real WLANs cannot achieve a time synchronization less than 800 ns (OFDM CP). As a result, conventional MIMO detectors such as minimum mean square error (MMSE) and zero-forcing (ZF) cannot decode the desired signal. In what follows, we first present a primer of conventional MMSE MIMO detector and then introduce an approximate-MMSE signal detector, which turns out to be capable of decoding the desired signals in the presence of unknown interference.

3.1 Conventional MMSE Detector

Consider one AP, say AP i, in the uplink transmission as shown in Figure 2. Denote $\mathbf{y} \in \mathbb{C}^{M \times 1}$ as the received signals at AP i, which includes both the desired signal from STA i and the interfering signals from other STAs. Denote $\mathbf{H} = [\mathbf{h}_1, \mathbf{h}_2, \cdots, \mathbf{h}_N]$ as the compound channel between AP i and all the STAs, where $\mathbf{h}_j \in \mathbb{C}^{M \times 1}$ is the channel between AP i and STA j. Denote $\mathbf{s} = [s_1 \ s_2 \cdots s_N]^T$ as the transmit signals at the N STAs, where s_i is the desired signal for AP i while others are the interfering signal for AP i. Denote $\mathbf{w} \in \mathbb{C}^{M \times 1}$ as the noise at AP i. Then, we have

$$y = Hs + w \tag{1}$$

If all the STAs had been perfectly synchronized in both time and frequency domains, then the signal detection problem (1) is equivalent to the point-to-point MIMO detection problem. In this case, the AP could first estimate the compound channel based on the orthogonal reference signals from the STAs and then decode its signals using MIMO detectors. For example, AP i can decode its desired signal in the presence of inter-STA interference using MMSE detector: $\mathbf{g}_i = \mathbf{i}_i \mathbf{H}^H (\mathbf{H}\mathbf{H}^H + \frac{\sigma_w^2}{\sigma_s^2} \mathbf{I})^{-1}$, where I is an identity matrix with proper dimension; \mathbf{i}_i is a row vector with 1 at the ith element and 0 at other elements, i.e., $\mathbf{i}_i = [0, \cdots, 0, 1, 0, \cdots 0]$; σ_s^2 is the signal power; and σ_w^2 is the noise power. It is easy to verify that when $\sigma_w = 0$, MMSE detector \mathbf{g}_i can perfectly recover the desired signal, i.e., $\hat{s}_i = \mathbf{g}_i \mathbf{y} = s_i$, where \hat{s}_i is the estimated version of s_i .

However, the required fine-grained synchronization (time offset less than the duration of OFDM CP and carrier frequency offset less than 350 Hz [2]) are not achievable in the existing WLANs due to the hardware limitation. For these reasons, uplink multi-user MIMO has been neither standardized nor commercialized in IEEE 802.11ac [18]. Therefore, we design a new detector to decode the desired signal at the APs.

3.2 An Approximate-MMSE Detector

We consider the signal detection in the absence of inter-STA synchronization. The main problem is that the AP are not able to estimate the channels due to the corrupted preamble in the packet.

As a result, the AP cannot construct the MMSE detector g_i , which requires the channel knowledge. In light of this, we consider how to construct the detector without the channel knowledge. To do so, we revisit the MMSE detector $g_i = i_i H^H (HH^H + \frac{\sigma_w^2}{\sigma_s^2} I)^{-1}$ and attempt to eliminate the channel H in its formula.

Let R_s denote the correlation of s, i.e., $R_s = \mathbb{E}[ss^H]$. Let R_w denote the correlation of w, i.e., $R_w = \mathbb{E}[ww^H]$. Then, we have

$$g_{i} = i_{i}H^{H}(HH^{H} + \frac{\sigma_{w}^{2}}{\sigma_{s}^{2}}I)^{-1}$$

$$\stackrel{(a)}{=} i_{i}R_{s}H^{H}(HR_{s}H^{H} + R_{w})^{-1}$$

$$= i_{i}\mathbb{E}[ss^{H}]H^{H}(H\mathbb{E}[ss^{H}]H^{H} + \mathbb{E}[ww^{H}])^{-1}$$

$$= \mathbb{E}[i_{i}ss^{H}H^{H}]\mathbb{E}[Hss^{H}H^{H} + ww^{H}]^{-1}$$

$$= \mathbb{E}[s_{i}(Hs)^{H}]\mathbb{E}[(Hs + w)(Hs + w)^{H}]^{-1}$$

$$\stackrel{(b)}{=} \mathbb{E}[s_{i}(Hs + w)^{H}]\mathbb{E}[(Hs + w)(Hs + w)^{H}]^{-1}$$

$$= \mathbb{E}[s_{i}y^{H}]\mathbb{E}[yy^{H}]^{-1}, \qquad (2)$$

where (a) follows from the fact that \mathbf{R}_s is full rank and (b) follows from the fact that $\mathbb{E}[s_i\mathbf{w}]=0$.

Eq. (2) shows that the MMSE detector can be computed without channel knowledge, but using $\mathbb{E}[s_iy^H]$ and $\mathbb{E}[yy^H]$. Now the question is how to compute these two terms. To address this question, we resort to an approximate approach by leveraging the reference symbols embedded into desired signals (e.g., preamble in 802.11 frame). Denote \mathcal{R} as the set of reference symbols embedded in the packet transmitted by STA i. Then, we have $\mathbb{E}[s_iy^H] \approx \frac{1}{|\mathcal{R}|} \sum_{(l,k') \in \mathcal{R}} s_i(l,k') y(l,k')^H$ and $\mathbb{E}[yy^H] \approx \frac{1}{|\mathcal{R}|} \sum_{(l,k') \in \mathcal{R}} y(l,k') y(l,k')^H$.

Denote $\mathbf{g}_i(k)$ as the approximate-MMSE signal detector for OFDM subcarrier k. We have

$$\mathbf{g}_{i}(k) = \left[\sum_{(l,k')\in\mathcal{R}} s_{i}(l,k')\mathbf{y}(l,k')^{\mathsf{H}}\right] \left[\sum_{(l,k')\in\mathcal{R}} \mathbf{y}(l,k')\mathbf{y}(l,k')^{\mathsf{H}}\right]^{+},$$
(3)

where $g_i(k)$ denotes the approximate-MMSE detector for subcarrier k; $s_i(l,k')$ is the reference symbols transmitted by STA i and y(l,k') is the received reference signal at AP i, both on OFDM symbol l and subcarrier k'; $[\cdot]^+$ is the Moore-Penrose inverse. It is noteworthy that y(l,k') in (3) is a blend of the reference signal from STA i and the interfering signals from other STAs.

We now summarize the approximate-MMSE detector as follows: For AP i, the detector first computes a row vector $\mathbf{g}_i(k)$ using (3), and then estimates the desired signal in the face of interference by computing $\hat{s}_i(l,k) = \mathbf{g}_i(k)\mathbf{y}(l,k)$, where l and k are the indexes of OFDM symbol and OFDM subcarrier, respectively.

For the approximate-MMSE detector, we have two remarks. Remark 1: It is evident that the approximate-MMSE detector in (3) does not require channel knowledge for signal detection. Instead, it uses the interfered reference signals in a packet to compute the linear detector directly. Therefore, the approximate-MMSE detector is well-suited to decode the signal in the face of unknown interference, while conventional MMSE detector is not capable of doing so.

Remark 2: For the approximate-MMSE detector, the reference signal symbols at the intended STA must be linearly independent

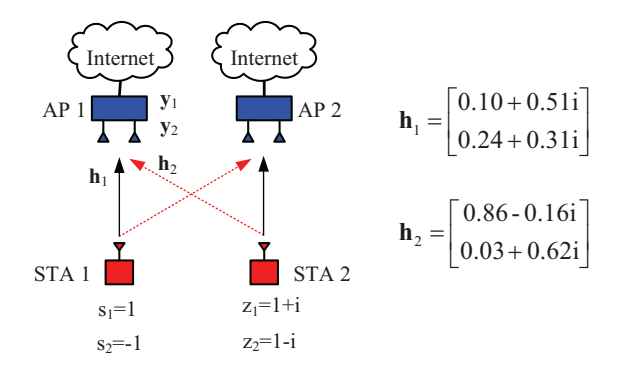


Figure 3: A small example to illustrate the performance of approximate-MMSE detector.

of the interfering signal symbols from the unintended STAs. Otherwise, equation (a) in (2) would not hold and, consequently, the approximate-MMSE detector could not decode the desired signal. This point will be further elaborated later.

3.3 An Example

We now use a small-sized network example to demonstrate the effectiveness of the proposed approximate-MMSE detector. Figure 3 shows the network example, and let us focus on AP 1. Let us assume that AP 1 does not know the channel knowledge (i.e., \mathbf{h}_1 and \mathbf{h}_2) and does not know the interfering signal at STA 2 (i.e., z_1 and z_2). AP 1 only knows the reference signals at STA 1 (i.e., $s_1 = 1$ and $s_2 = -1$). Suppose that the noise is negligible. Then, the received signals at AP 1 can be written as: $\mathbf{y}_1 = \begin{bmatrix} 1.12 + 1.21i, & -0.35 + 0.96i \end{bmatrix}^\mathsf{T}$ and $\mathbf{y}_2 = \begin{bmatrix} 0.60 - 1.53i, & 0.41 + 0.28i \end{bmatrix}^\mathsf{T}$.

At AP 1, according to (3), the approximate-MMSE detector can be constructed by:

$$g_1 = [s_1 \mathbf{y}_1^{\mathsf{H}} + s_2 \mathbf{y}_2^{\mathsf{H}}] [\mathbf{y}_1 \mathbf{y}_1^{\mathsf{H}} + \mathbf{y}_2 \mathbf{y}_2^{\mathsf{H}}]^+$$

= [-0.3191 - 1.0047*i* 1.3420 - 0.6369*i*]. (4)

Surprisingly, the constructed detector has $g_1h_1 = 1$ and $g_1h_2 = 0$. This means the constructed approximate-MMSE detector at AP 1 can completely cancel interference from STA 2 and perfectly equalize the channel distortion. Simply put, it can perfectly recover the desired signal in the presence of unknown interference. From this example, we have two observations on the approximate-MMSE detector. First, the reference signals at the two STAs cannot be identical. Otherwise, AP 1 cannot decode its desired signal. In this example, it is easy to verify that, when $z_1 = s_1 = 1$ and $z_2 = s_2 = -1$, $\mathbf{g}_1\mathbf{h}_1 \neq 1$ and $\mathbf{g}_1\mathbf{h}_2 \neq 0$. As we will see in the next section, a tricky protocol will be designed for TCCI to ensure that the reference signal and interference are linearly independent. Second, fine-grained synchronization among all the STAs is not needed. This is because the construction of approximate-MMSE detector is independent of the interference. It can be verified in this example that, when z_1 and z_2 are any random numbers, AP 1 can still decode its desired signals in the face of interference.

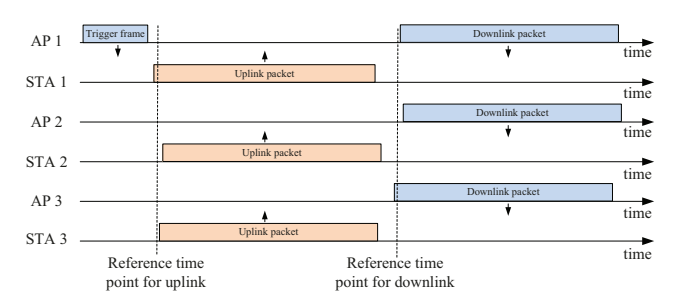


Figure 4: A MAC protocol for concurrent transmission among multiple WLANs. Colored boxes represent the transmission of data packets.

4 TCCI: A CO-CHANNEL INTERFERENCE MANAGEMENT SCHEME

In this section, we present TCCI, a practical scheme to tame the cochannel interference using AP's multiple antennas, which in turn enable concurrent transmission in WLANs. TCCI comprises a new protocol and a new PHY design. In what follows, we first present the new MAC protocol and then elaborate on the corresponding PHY design based on the above approximate-MMSE detector.

4.1 MAC Protocol

Referring to Figure 2, we assume that one of the APs has been selected as lead AP, and the lead AP then obtains network topology information including the number of coexisting APs, the number of antennas on each AP, and the set of STAs served by each AP. In reality, the lead AP can obtain such information from the gateway via its Ethernet connection. Based on the network topology information, the lead AP selects a subset of APs and a subset of STAs for concurrent data transmission. For these WLANs, Figure 4 shows the MAC protocol for TCCI, which is detailed as follows:

Step 1: *Trigger Frame.* The lead AP broadcasts an announcement packet for concurrent transmission. This packet includes the announcement command, the addresses of the participating APs and STAs, the length of uplink/downlink packets, and other necessary information.

Step 2: *Uplink Transmission*. Upon receiving the announcement packet, the selected STAs send their packets to their respective APs. The uplink transmission comprises an array of consecutive signal frames, each of which is assembled using the 802.11 frame format as shown in Figure 5. Details of this step are presented in §4.2.

Step 3: Downlink Transmission. Once completing the reception of uplink packets, each AP sends the packet to its serving STAs in the downlink. Again, the downlink comprises an array of consecutive signal frames, each of which is assembled using 802.11 frame in Figure 5. Details of this step are presented in §4.3.

Step 4: *Repetition.* The network repeats Steps 2 and 3 until the defined number of transmissions is reached. The number of transmissions is defined in the trigger frame.

In Step 2, supposedly, each STA transmits its data packet after a predefined amount of time (e.g., Short Interframe Space or SIFS). The time point that the STAs are supposed to transmit their packets



Figure 5: The 802.11 frame structure used for data transmission.

is marked as "reference time point for uplink" in Figure 4. In real systems, due to the imperfection of circuit and clocking, various delays may affect the start point of the STAs' packet transmission. The time misalignment of those uplink packets cannot be adjusted within the time duration of OFDM CP, which is 0.8 μs in 802.11ac [18]. Due to the time misalignment, the uplink packets constitute interference for each other. On the other hand, the time misalignment is always less than SIFS (16 μs), which is equivalent to the time duration of 4 OFDM symbols. The same thing occurs in Step 3, where the downlink packets from the APs are very likely to be misaligned in time, as illustrated in Figure 4.

It is worth pointing out that we use the 802.11 frame in Figure 5 for uplink and downlink transmission because we intend to preserve the backward compatibility of our scheme. As we will show via experiments, through a tricky protocol design and a modification of NIC driver, TCCI can enable concurrent transmission for COTS Atheros Wi-Fi dongles.

4.2 Uplink Transmission

In the phase of uplink transmission as shown in Figure 4, each of the selected STAs sends its packet to its serving AP. In our design, the packet comprises an array of consecutive signal frames as shown in Figure 5. However, due to the broadcast nature of wireless medium, those transmitted packets collide in the air. At each AP, to decode its desired packet in the presence of interference, we use the approximate-MMSE detector presented in the previous section. While the idea is straightforward, decoding the packet still faces the following two challenges.

Challenge 1 – Identical Reference Symbols: In the uplink transmission, we use the approximate-MMSE detector at each AP to decode the signal from its serving STA in the presence of interference from other STAs. As we pointed out in § 3, the reference sequence must be linearly independent of the corresponding interference sequences. Otherwise, the approximate-MMSE detector cannot successfully decode the desired signal in the face of interference.

Fulfilling this requirement, however, is a challenging task. This is because all the nodes in the network use the same frame structure, which has the same preamble (reference symbols) for the construction of approximate-MMSE detector. In reality, there is a possibility that the time misalignment of the packets from two different STAs is less than OFDM CP, as illustrated in Figure 6(a). In this case, neither AP 1 nor AP 2 can decode its desired signal using the proposed approximate-MMSE detector. This is because the two APs cannot differentiate the two preambles in the spatial domain and, as a result, the constructed approximate-MMSE detector cannot cancel the interference and equalize the channel distortion. Therefore, ensuring the independence of reference symbols at each AP is a challenging task.

Challenge 2 – Time Misalignment: In real networks, the time misalignment of the packets from different STAs can also be larger

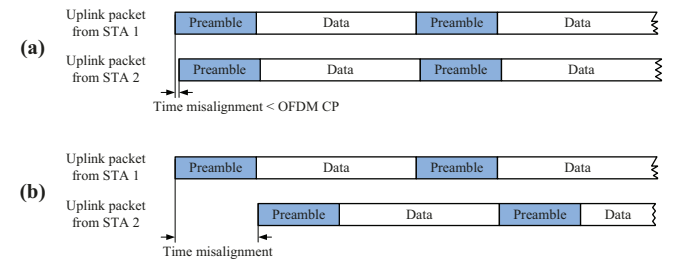


Figure 6: Possible time misalignment patterns of two uplink packets. (a) time misalignment is less than OFDM CP. (b) time misalignment is larger than preamble.

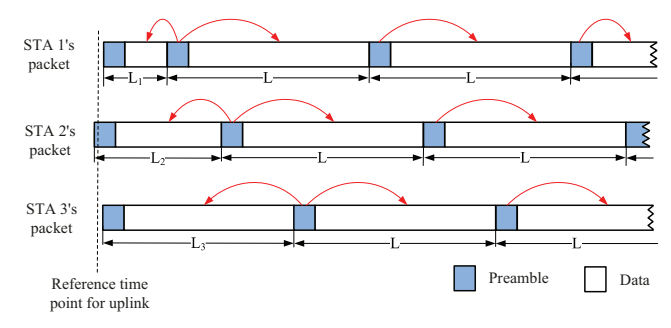


Figure 7: Illustrating our approach to ensure success of signal detection by controlling the time duration of STAs' first frame.

than the time duration of preamble as shown in Figure 6(b). In such a case, AP 2 is capable of decoding the signal frame from STA 2. However, AP 1 cannot decode the first signal frame from STA 1. This is because the preamble of STA 1's first frame is not interfered by the interference while its data part is interfered by STA 2's signal. To ensure the success of uplink, such a case must be handled, which is another challenging task.

Our Approach: Recall that each STA's uplink packet comprises an array of consecutive frames, each of which has two parts: preamble and payload, as shown in Figure 5. Our approach to addressing the above two challenges is by controlling the time duration of each STA's uplink frames. Figure 7 illustrates the basic idea of our approach. For all the STAs, the time duration of the first frame is unique, while the time duration of other frames are the same. Specifically, in the uplink transmission, let L_i denote the number of OFDM symbols in STA i's first frame; let L denote the number of OFDM symbols in STA i's other frames. Then, we let $L_i = 12i$, $1 \le i \le N$. Recall that the time duration of preamble is 4 OFDM symbols. The increment step is equal to the triple of preamble duration. For L, its value can be freely set, and we let L = 40 in our experiments.

Frame Detection at AP: As shown in Figure 7, the length adjustment of the first frame avoids the preamble collision for all frames except the first one. That is, for all frames except the first one, their preambles will not overlap with another preamble, but overlap with a segment of data. This is guaranteed, because the time misalignment is always less than 16 μ s (equivalent to 4 OFDM symbols). To decode those frames, the APs can employ the approximate-MMSE detector in (3). By using the interfered preamble as the reference

symbols, the constructed approximate-MMSE detector can decode its desired signal in the presence of co-channel interference.

A remaining question is how to decode the first frame in the uplink packet. As shown in Figure 7, the length adjustment of the first frame cannot avoid the preamble collision for the first frames. There is a high probability of the first preambles overlapping with each other. Our solution to this problem is that the first frame uses the second frame's preamble to construct the approximate-MMSE detector for signal detection. This idea is shown in Figure 7. Since it is guaranteed that the second preamble is interfered by the payload data, the constructed approximate-MMSE detector is capable of decoding the first frame in the presence of interference.

4.3 Downlink Transmission

We now focus on the concurrent downlink transmission in the proposed protocol in Figure 4. The key technique to enable concurrent downlink transmission is beamforming. Recall that the number of AP's antennas is greater than or equal to the number of STAs $(M \geq N)$. Using the spatial degrees of freedom provided by its antennas, each AP can steer its signal to its intended STA and precancel its generated interference for its unintended STAs. If the AP has global channel knowledge between itself and all the STAs, then beamforming becomes a trivial task. However, with limited cooperation among the APs, global channel knowledge is not available to each individual AP. The key challenge lies in the design of beamforming filters for concurrent downlink transmission without global channel knowledge.

To address this challenge, we take advantage of channel reciprocity. For an over-the-air wireless MIMO channel between all the STAs and an AP, if its uplink transfer function can be expressed as H, then its downlink transfer function can be written as H^T. Based on this fact, we can use the approximate-MMSE detector g_i computed in the uplink as the beamforming filter p_i in the downlink, i.e., $\mathbf{p}_i = \alpha_i \mathbf{g}_i^\mathsf{T}$, where *i* is index of AP and coefficient α_i is used to meet the transmit power requirement at AP i. Suppose that the approximate-MMSE detector \mathbf{g}_i can perfectly recover the desired signal in the uplink as we have shown in the example in §3.3, i.e., $g_iH = i_i$, $1 \le i \le N$. Then, the downlink transmission can be expressed as $\mathbf{H}^\mathsf{T} \mathbf{p}_i$. Furthermore, we have $\mathbf{H}^\mathsf{T} \mathbf{p}_i = \alpha_i \mathbf{H}^\mathsf{T} \mathbf{g}_i^\mathsf{T} = \alpha_i [\mathbf{g}_i \mathbf{H}]^\mathsf{T} = \alpha_i \mathbf{i}_i^\mathsf{T}$. This indicates that using beamforming filter $\mathbf{p}_i = \alpha_i \mathbf{g}_i^\mathsf{T}$, AP *i* can completely pre-cancel the interference for its unintended STAs. As a result, the N APs can serve their respective STAs as if there were no co-channel interference.

While the idea of this beamforming method is straightforward, one problem remains unsolved. That is, in real wireless systems, the wireless channel is compound. It includes not only the effect of over-the-air wireless channel but also the effects of Tx/Rx RF circuits. While the over-the-air channels are reciprocal, the Tx/Rx RF circuits are typically not. One approach to address this issue is channel calibration, which measures the discrepancy between Tx and Rx RF circuits of each transceiver and compensates for their discrepancy. This approach, however, is too complex for implementation. Considering that the STAs have a single antenna, we can employ relative channel calibration, which only needs to compensate the Tx/Rx RF circuit at the APs (no need to compensate for

the STAs). In our experiments, we implement the relative channel calibration algorithm in [28] at the APs for beamforming in the downlink transmission.

4.4 Discussions

Compatibility with 802.11 Client Devices: TCCI can work with legacy 802.11 PHY layer, but cannot work with legacy 802.11 MAC protocol. This is because legacy 802.11 MAC protocol is based on carrier sensing, which will prevent concurrent transmission from multiple Wi-Fi devices. Fortunately, many existing Wi-Fi devices (e.g., laptops and smartphones) can temporarily disable their carrier sensing for concurrent uplink transmission by modifying their drivers or firmwares. The carrier sensing functionality can be immediately enabled after the completion of the uplink packet transmission. As we will show in our experiments, TCCI enables concurrent transmission between our custom-built APs and COTS Atheros Wi-Fi dongles with a modified Linux driver. Taking advantage of this opportunity, TCCI can serve many incumbent Wi-Fi client devices by updating their drivers.

No Need of Synchronization and Data Sharing: It is evident that TCCI does require neither inter-STA nor inter-AP fine-grained synchronization. Moreover, TCCI does not require data sharing among the APs and does not require channel information exchange among the APs. These features make it amenable to practical implementation.

5 IMPLEMENTATION AND EXPERIMENTAL SETUP

5.1 Implementation

We have built a prototype of TCCI on a wireless testbed that consists of USRP devices and COTS Qualcomm Atheros 802.11n dongles. In what follows, we present the implementation of STAs and APs, respectively.

STA Devices: For the STAs, we use Alfa AWUS036NHA Wireless USB Adapters as shown in Figure 8(b), which are built using Qualcomm Atheros AR9271 chipset and support IEEE 802.11b/g/n [24]. We have modified its open-source firmware (modwifi-ath9k-htc in [25]) to temporarily disable carrier sense, RTS/CTS, and ACK for uplink transmission. We also set SIFS/AIFS to its minimum. Meanwhile, we modified Linux 802.11 ath9k driver in Linux to implement the protocol in Figure 4. Our modified version can be found on GitHub [31]. Particularly, for the first frame in the uplink packet, we set the number of its OFDM symbols as shown in Figure 7. For the uplink packet, we fix the MCS index to 2, which corresponds to QPSK modulation, 3/4 coding rate, and 18 Mbps data rate. We also set channel bandwidth to 20 MHz and guard interval (OFDM CP) to 800 ns. The transmit power is set to its maximum (~ 20 dBm), and the carrier frequency is set to 2.427 GHz (channel 4). Light interference from incumbent Wi-Fi networks was observed in this channel during our experiments.

While using the COTS dongles is good to demonstrate the compatibility of TCCI with commercial devices, it is hard to measure the performance of the downlink transmission. This is because Atheros AR9271 chipset does not provide information of PHY-layer signal detection. Therefore, we also implement the STAs using USRP N210 devices. For ease of experimentation and to avoid USRP's



Figure 8: Floor plan and network devices.

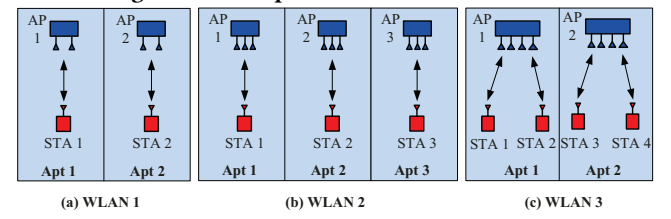


Figure 9: Experimental setup for performance evaluation.

Table 1: EVM specification in IEEE 802.11ac standards [18].

EVM (dB)	(inf -5)	[-5 -10)	[-10 -13)	[-13 -16)	[-16 -19)	[-19 -22)
Modulation	N/A	BPSK	QPSK	QPSK	16QAM	16QAM
Coding rate	N/A	1/2	1/2	3/4	1/2	3/4
γ (EVM)	0	0.5	1	1.5	2	3
EVM (dB)	[-22 -25)	[-25 -27)	[-27 -30)	[-30 -32)	[-32 -inf)	
Modulation	64QAM	64QAM	64QAM	256QAM	256QAM	
Coding rate	2/3	3/4	5/6	3/4	5/6	
γ (EVM)	4	4.5	5	6	20/3	

re-sampling CIC, we set the sampling rate to 5 MHz. Using the custom-built STAs, we are able to measure the EVM of the demodulated signals in the downlink.

AP Devices: We build the APs using USRP N210 devices. We connect multiple USRP N210 devices together using an external clock so that it works in MIMO mode, as shown in Figure 8(c). The custombuilt APs can support up to four antennas for radio signal transmission and reception. On the APs, we implement our proposed signal detection and beamforming methods at the PHY layer as well as the proposed MAC protocol in Figure 4.

Real-Time Testbed: The custom-built APs and the two types of STAs (Wi-Fi dongles and custom-built STAs) constitute a real-time wireless system testbed to evaluate the performance of TCCI. To realize the real-time communication, we implement the PHY-layer signal processing modules and the MAC-layer protocol in C++. When building the APs on the USRP devices, the engineering challenge lies in using the same antenna for transmission and reception as well as setting a proper delay time for TX/RX switch. To address this challenge, we implement the USRP interface in C++ to control USRP TX/RX switch by our MAC protocol. In our system, the Tx/Rx switch time is about 500 ms, and channel coding (LDPC) is not implemented on the APs.

5.2 Experimental Setup

Figure 9 shows our experimental setup for performance evaluation. Specifically, we consider three WLANs: (i) two APs serve two STAs; (ii) three APs serve three STAs; and (iii) four APs serve four STAs. Figure 9 shows the deployment locations for the APs and STAs in our tests.

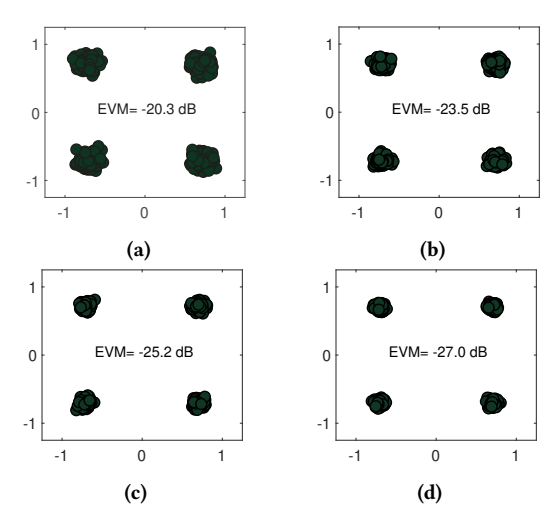


Figure 10: (a) Demodulated signal at AP 1 in coexisting scenario. (b) Demodulated signal at AP 2 in coexisting scenario. (c) Demodulated signal at AP 1 in interference-free scenario. (d) Demodulated signal at AP 2 in interference-free scenario.

6 PERFORMANCE EVALUATION

In this section, we evaluate the performance of TCCI on the wireless testbed.

6.1 Performance Baseline and Metrics

Performance Baseline: We use the TDMA protocol (a interference avoidance scheme) as the comparison baseline. In this protocol, different APs are assigned into different time slots so that the network has no co-channel interference.

Performance Metrics: We measure the performance of TCCI using two metrics. The first one is error vector magnitude (EVM), which can be mathematically written as:

$$EVM (dB) = 10 \log_{10}(\frac{\mathbb{E}(|X - \hat{X}|^2)}{\mathbb{E}(|X|^2)}),$$
 (5)

where X is the original signal and \hat{X} is the estimated signal. The second performance metric that we use is data rate, which is extrapolated by $r=\frac{48}{80}\times b\times \gamma(\text{EVM})$ Mbps, where 48 is the number of subcarriers used for payload in an OFDM symbol, 80 is the length of one OFDM symbol (including CP), b is the sample rate (in Msps), and $\gamma(\text{EVM})$ is the average number of bits carried by one subcarrier and its values are given in Table 1. In our experiments, b=20 when the STAs are commercial Wi-Fi dongles and b=5 when the STAs are custom-built using USRP devices.

6.2 A Case Study

In this case study, we consider WLAN 1 in Figure 9 and use commercial Wi-Fi dongles as the STAs. We place the two dongles at locations L_1 and L_2 in Figure 8(a).

Uplink: In the uplink, each AP demodulates the signal from its serving dongle in the presence of co-channel interference from the other dongle. Figure 10(a) and (b) present the constellation of the demodulated signals at the two APs when TCCI is used. The EVMs achieved by the two APs are -20.3 dB and -23.5 dB. The

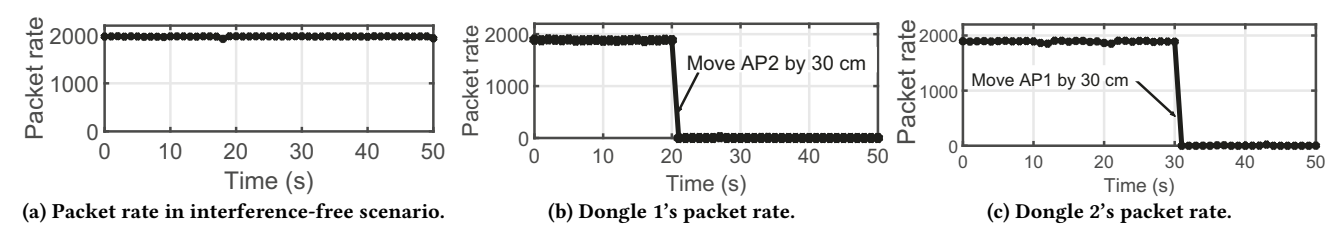
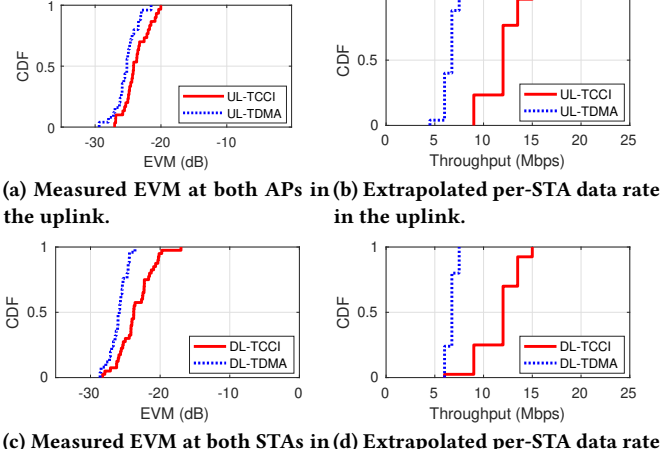


Figure 11: Observed packet rate from Wireshark in the case study.



(c) Measured EVM at both STAs in (d) Extrapolated per-STA data rate the downlink. in the downlink.

Figure 12: Distribution of measured EVM and extrapolated per-STA throughput in WLAN 1.

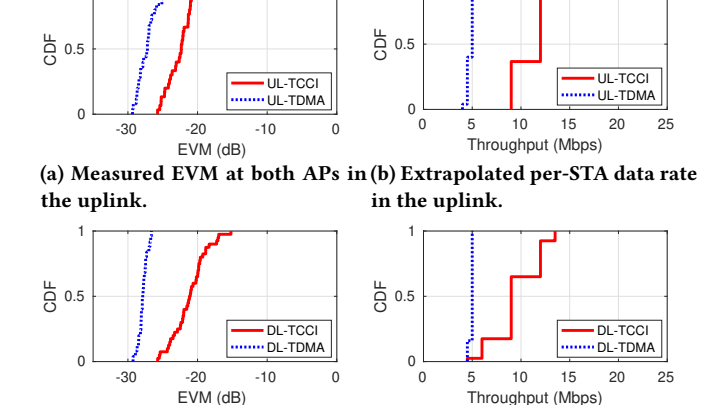
extrapolated data rates for AP 1 and AP 2 are 9 Mbps and 12 Mbps, respectively.

In contrast, Figure 10(c) and (d) present the constellation of the demodulated signals at the two APs when TDMA is used (i.e., interference-free case). The EVMs achieved by the two APs are $-25.2~\mathrm{dB}$ and $-27.0~\mathrm{dB}$. In TDMA mode, since each of the two APs can use a half of the airtime for communication, the extrapolated data rate should be divided by two. Therefore, the data rates achieved by AP 1 and AP 2 are 6.8 Mbps and 7.5 Mbps, respectively. Obviously, TCCI outperforms TDMA.

Downlink: In the downlink, each dongle receives data packets from its serving AP in the presence of co-channel interference from the other AP. Unfortunately, we are not able to access the demodulated signal at the commercial Wi-Fi dongles and thus cannot plot the constellation. Therefore, we use Wireshark, which is an open-source packet analyzer software [32], to monitor the packet reception at the two dongles.

Figure 11 plots the monitoring results from Wireshark. Specifically, Figure 11(a) shows the interference-free case. In this case, AP 1 sends data packet to STA 1 (dongle 1); AP 2 and STA 2 are deactivated. There is no co-channel interference in the network. From the figure, we can see that the achieved packet rate is about 1960 packets per second in the interference-free scenario. This number will be used as the benchmark.

Figure 11(b) and (c) show the packet reception rate at the two dongles in the coexisting scenario. In this scenario, our beamforming method has been employed at the two APs for downlink transmission. At the moment of 20s, we move the location of AP 2 by a



(c) Measured EVM at both STAs in (d) Extrapolated per-STA data rate the downlink. in the downlink.

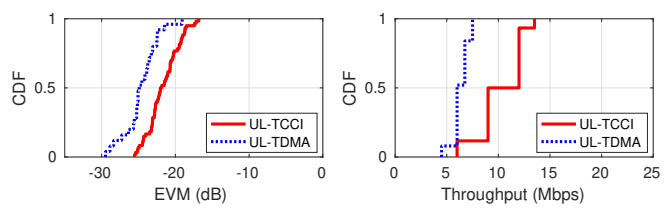
Figure 13: Distribution of measured EVM and extrapolated per-STA throughput in WLAN 2.

distance of 30 cm. At the moment of 30s, we move the location of AP 1 by a distance of 30 cm. From the figures we can see that, with our beamforming method, both dongles can successfully decode the signals at a rate of 1905 packets per second. The achieved packet rate is almost the same as that of the interference-free scenario. This indicates that the co-channel interference is pre-canceled by the two APs. When we move AP 2 by 30 cm, its beamforming filters are not effective any more. As a result, the co-channel interference occurs at dongle 1, and its packet rate drops to almost 0, as shown in the figure. When we move AP 1 by 30 cm, the same phenomenon is observed at dongle 2. This shows the effectiveness of our proposed beamforming method.

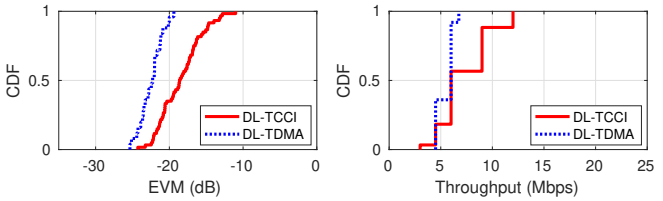
6.3 EVM and Throughput

We now measure the performance of TCCI in the three networks in Figure 9 by placing the STAs throughout the 25 locations in Figure 8. We use 5 Msps sample rate in these tests.

WLAN 1: As shown in Figure 9(a), this network has two APs and two STAs. Figure 12(a) and (b) plot the measured EVM and extrapolated throughput in the uplink. Specifically, Figure 12(a) shows the measured EVMs of the demodulated signals at the two APs. The average EVM achieved by TCCI is -23.7 dB. In contrast, the average EVM achieved by TDMA is -25.2 dB. The EVM gap between TCCI and TDMA is about 1.5 dB on average. Based on the measured EVM, we extrapolate the per-STA data rate (throughput). Figure 12(b) presents the extrapolated uplink per-STA throughput. The average per-STA throughput achieved by TCCI and TDMA are 11.7 Mbps



(a) Measured EVM at both APs in (b) Extrapolated per-STA data rate the uplink. in the uplink.



(c) Measured EVM at both STAs in (d) Extrapolated per-STA data rate the downlink. in the downlink.

Figure 14: Distribution of measured EVM and extrapolated per-STA throughput in WLAN 3.

and 6.5 Mbps. It offers 80% throughput gain compared to TDMA in the uplink.

Figure 12(c) and (d) plot the measured EVM and extrapolated throughput in the downlink. The average EVMs achieved by TCCI and TDMA are -23.5 dB and -26.0 dB. The EVM gap of the two schemes is about 3.5 dB. The average per-STA throughput achieved by TCCI and TDMA are 11.7 Mbps and 6.7 Mbps. Clearly, TCCI improves the STAs' throughput by 75% compared to TDMA in the downlink.

WLAN 2: Figure 13 plots the measured EVM and extrapolated per-STA throughput in the network as shown in Figure 9(b). In the uplink, TCCI achieves an average of −22.7 dB EVM, and its gap with TDMA is about 4.5 dB. The average per-STA throughput achieved by TCCI and TDMA are 11.1 Mbps and 4.8 Mbps. It offers 131% throughput gain compared to TDMA in the uplink. In the downlink, TCCI achieves an average of −21.1 dB EVM, and its gap with TDMA is about 6.7 dB. The average per-STA throughput achieved by TCCI and TDMA are 9.6 Mbps and 4.9 Mbps. It offers 96% throughput gain compared to TDMA in the downlink.

WLAN 3: Figure 14 plots the measured EVM and extrapolated per-STA throughput in the network as shown in Figure 9(c). In the uplink, TCCI achieves an average of −21.6 dB EVM, and its gap with TDMA is about 3 dB. The average per-STA throughput is 10.3 Mbps. It offers 61% throughput gain compared to TDMA, which yields 6.4 Mbps per-STA throughput. In the downlink, TCCI achieves an average of −18.5 dB EVM, and its gap with TDMA is about 4 dB. The average per-STA throughput achieved by TCCI and TDMA are 7.3 Mbps and 5.5 Mbps. It offers 33% throughput gain compared to TDMA in the downlink.

Summary of Observations: Figure 15 presents the throughput comparison between TCCI and TDMA. It is evident that TCCI can enable concurrent transmission for multiple coexisting APs. The throughput gain of TCCI over TDMA is 77% in WLAN 1, 113% in WLAN 2, and 50% in WLAN 3. More importantly, TCCI enhances network fairness as the APs can provide services all the time.

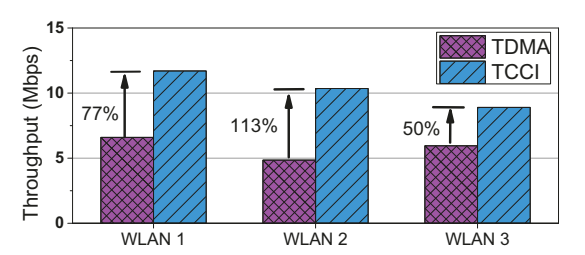


Figure 15: Throughput comparison between TCCI and TDMA.

7 RELATED WORK

In this section, we briefly review the interference management techniques for WLANs.

Interference Avoidance: Despite the over-half-century evolution of wireless technology, interference avoidance is still the dominant interference management paradigm in wireless networks. This can be attributed to its simplicity in practical implementation. Different techniques have been developed to avoid interference while maximizing network throughput, such as CSMA [4], TDMA [33], and OFDMA [8]. CSMA is the MAC protocol in incumbent WLANs (802.11a/b/g/n/ac), while OFDMA will be adopted for the next-generation Wi-Fi (802.11ax [21]). Meanwhile, TDMA-based centralized schedulers (e.g., [6, 7, 9, 10, 23]) have also been studied for WLANs to maximize network throughput.

Interference Exploitation: While interference avoidance techniques are easy to implement, their limitation is also obvious. That is, only one AP can be active at a time, and the network throughput is limited by co-channel interference. To overcome this limitation, interference exploitation paradigm was proposed. In the past decades, a large body of work has been done in this area, such as interference cancellation [11, 13, 19, 36], interference alignment [1], network MIMO [3, 27, 30, 37, 38], and collision recovery [12]. All these works require transmitter-side tight synchronization for interference management. Such transmitter-side tight synchronization, however, is not achievable in distributed WLANs.

Clock and Time Synchronizations: Network-wide synchronization is one of the barriers facing the management of co-channel interference. Research efforts (see, e.g., [2, 14, 16, 17, 22, 26, 29]) have invested on achieving global synchronization so that all the network nodes form a large-scale MU-MIMO, where the co-channel interference can be easily handled. For example, [16] proposed a layering protocol called Chorus to achieve network-wide clock and time synchronization for LTE systems. [26] proposed a distributed architecture called SourceSync to achieve synchronization for diversity exploitation. [2] analyzed time and clock synchronizations in large-sized dense wireless networks. However, these works cannot achieve the required accuracy of time synchronization for uplink transmission in practical WLANs.

This Work: This work differs from the body of existing work as it does not require inter-user fine-grained synchronization to tame co-channel interference. Moreover, it is amenable to practical implementation and compatible with COTS 802.11 devices.

8 CONCLUSION

In many real-world WLANs, network-wide fine-grained time synchronization is not achievable due to the hardware limitation, and inter-network data sharing is not permitted due to the privacy concern. These observations motivated us to design a new concurrent transmission scheme that requires neither fine-grained synchronization nor inter-network data sharing. In this paper, we proposed TCCI, a holistic scheme to enable concurrent transmission for WLANs in the absence of fine-grained synchronization and data sharing. The enabling technique of TCCI is a new detection and beamforming method for a multi-antenna AP, which can tame unknown interference without channel knowledge. We have built a prototype of TCCI on a wireless testbed and demonstrated its compatibility with commercial 802.11 devices. Our experimental results showed that TCCI can achieve up to 113% throughput gain compared to a TDMA-based interference avoidance scheme.

REFERENCES

- Fadel Adib, Swarun Kumar, Omid Aryan, Shyamnath Gollakota, and Dina Katabi. 2013. Interference alignment by motion. In Proc. of the 19th annual international conference on Mobile computing & networking. 279–290.
- [2] Maria Antonieta Alvarez and Umberto Spagnolini. 2018. Distributed time and carrier frequency synchronization for dense wireless networks. IEEE Transactions on Signal and Information Processing over Networks 4, 4 (2018), 683–696.
- [3] Horia Vlad Balan, Ryan Rogalin, Antonios Michaloliakos, Konstantinos Psounis, and Giuseppe Caire. 2012. Achieving high data rates in a distributed MIMO system. In Proc. of the 18th annual international conference on Mobile computing and networking. 41–52.
- [4] Giuseppe Bianchi, Luigi Fratta, and Matteo Oliveri. 1996. Performance evaluation and enhancement of the CSMA/CA MAC protocol for 802.11 wireless LANs. In Proceedings of PIMRC'96-7th International Symposium on Personal, Indoor, and Mobile Communications, Vol. 2. 392–396.
- [5] Zhe Chen, Xu Zhang, Sulei Wang, Yuedong Xu, Jie Xiong, and Xin Wang. 2017. BUSH: Empowering large-scale MU-MIMO in WLANs with hybrid beamforming. In IEEE INFOCOM 2017-IEEE Conference on Computer Communications. IEEE, 1–0
- [6] Robson Costa, Jim Lau, Paulo Portugal, Francisco Vasques, and Ricardo Moraes. 2019. Handling real-time communication in infrastructured IEEE 802.11 wireless networks: The RT-WiFi approach. Journal of Communications and Networks 99 (2019), 1–15.
- [7] Robson Costa, Paulo Portugal, Francisco Vasques, and Ricardo Moraes. 2010. A TDMA-based mechanism for real-time communication in IEEE 802.11 e networks. In Proc. of IEEE 15th Conference on Emerging Technologies & Factory Automation (ETFA 2010). 1–9.
- [8] Der-Jiunn Deng, Ying-Pei Lin, Xun Yang, Jun Zhu, Yun-Bo Li, Jun Luo, and Kwang-Cheng Chen. 2017. IEEE 802.11 ax: Highly efficient WLANs for intelligent information infrastructure. IEEE Communications Magazine 55, 12 (2017), 52–59.
- [9] Petar Djukic and Prasant Mohapatra. 2009. Soft-TDMAC: A software TDMAbased MAC over commodity 802.11 hardware. In Proc. of IEEE INFOCOM. 1836– 1844.
- [10] Petar Djukic and Shahrokh Valaee. 2009. Delay aware link scheduling for multihop TDMA wireless networks. IEEE/ACM Transactions on Networking 17, 3 (2009), 870–883
- [11] Shyamnath Gollakota, Fadel Adib, Dina Katabi, and Srinivasan Seshan. 2011. Clearing the RF smog: making 802.11 n robust to cross-technology interference. In ACM SIGCOMM Computer Communication Review, Vol. 41. 170–181.
- [12] Shyamnath Gollakota and Dina Katabi. 2008. Zigzag decoding: Combating hidden terminals in wireless networks. Vol. 38. ACM.
- [13] Shyamnath Gollakota, Samuel David Perli, and Dina Katabi. 2009. Interference alignment and cancellation. In Proc. of ACM SIGCOMM Computer Communication Review, Vol. 39. 159–170.
- [14] Malik Muhammad Usman Gul, Xiaoli Ma, and Sungeun Lee. 2014. Timing and frequency synchronization for OFDM downlink transmissions using Zadoff-Chu sequences. IEEE Transactions on Wireless Communications 14, 3 (2014), 1716–1729.
- [15] Ezzeldin Hamed, Hariharan Rahul, Mohammed A Abdelghany, and Dina Katabi. 2016. Real-time distributed MIMO systems. In Proceedings of the 2016 ACM SIGCOMM Conference. ACM, 412–425.
- [16] Ezzeldin Hamed, Hariharan Rahul, and Bahar Partov. 2018. Chorus: Truly distributed distributed-MIMO. In Proc. of the 2018 Conference of the ACM Special Interest Group on Data Communication. 461–475.

- [17] Yao-Win Hong and Anna Scaglione. 2005. A scalable synchronization protocol for large scale sensor networks and its applications. *IEEE Journal on Selected Areas in Communications* 23, 5 (2005), 1085–1099.
- [18] IEEE 802.11ac. 2014. IEEE Standard for Information technology Local and metropolitan area networks Part 11: Wireless LAN Medium Access Control (MAC) and Physical Layer (PHY) Specifications Amendment 5: Enhancements for Higher Throughput. IEEE Standards 802.11ac (2014).
- [19] Sachin Katti, Shyamnath Gollakota, and Dina Katabi. 2007. Embracing wireless interference: Analog network coding. In Proc. of ACM SIGCOMM Computer Communication Review, Vol. 37. 397–408.
- [20] Ruizhi Liao, Boris Bellalta, Miquel Oliver, and Zhisheng Niu. 2014. MU-MIMO MAC protocols for wireless local area networks: A survey. IEEE Communications Surveys & Tutorials 18, 1 (2014), 162–183.
- [21] Shangjuan Lin, Hang Qi, Xiangming Wen, Zhaoming Lu, and Zhiqun Hu. 2018. An Efficient Group-Based OFDMA MAC Protocol for Multiuser Access in Dense WLAN Systems. In Proc. of IEEE International Conference on Communications Workshops (ICC Workshops). 1–6.
- [22] Ali A Nasir, Hani Mehrpouyan, Steven D Blostein, Salman Durrani, and Rodney A Kennedy. 2011. Timing and carrier synchronization with channel estimation in multi-relay cooperative networks. *IEEE Transactions on Signal Processing* 60, 2 (2011), 793–811.
- [23] Xiaoqi Qin, Xu Yuan, Zhi Zhang, Feng Tian, Thomas Hou, and Wenjing Lou. 2019. Joint User-AP Association and Resource Allocation in Multi-AP 60 GHz WLAN. IEEE Transactions on Vehicular Technology (2019).
- [24] Qualcomm Atheros. [n.d.]. AR9271 Highly integrated single-chip USB with 802.11n support. www.ath-drivers.eu/qualcomm-atheros-datasheets-for-AR9271.html [Online; accessed 28-Jul-2019] ([n.d.]).
- [25] Qualcomm Atheros. [n.d.]. open-ath9k-htc-firmware. https://github.com/vanhoefm/modwifi-ath9k-htc [Online; accessed 28-Jul-2019] ([n.d.]).
- [26] Hariharan Rahul, Haitham Hassanieh, and Dina Katabi. 2011. SourceSync: A distributed wireless architecture for exploiting sender diversity. ACM SIGCOMM Computer Communication Review 41, 4 (2011), 171–182.
- [27] Hariharan Shankar Rahul, Swarun Kumar, and Dina Katabi. 2012. JMB: Scaling wireless capacity with user demands. In Proc. of the ACM SIGCOMM 2012 conference on Applications, technologies, architectures, and protocols for computer communication. 235–246.
- [28] Clayton Shepard, Hang Yu, Narendra Anand, Erran Li, Thomas Marzetta, Richard Yang, and Lin Zhong. 2012. Argos: Practical many-antenna base stations. In Proc. of ACM International Conference on Mobile Computing and Networking (MobiCom). 53–64.
- [29] Wen-Qin Wang. 2014. Carrier frequency synchronization in distributed wireless sensor networks. IEEE Systems Journal 9, 3 (2014), 703–713.
- [30] Teng Wei and Xinyu Zhang. 2016. Random access signaling for network MIMO uplink. In IEEE INFOCOM 2016-The 35th Annual IEEE International Conference on Computer Communications. 1–9.
- [31] Wireless Systems Laboratory. 2019. Co-channel Interference Management. https://https://github.com/wsl216/cochnlnterference [Online; accessed 13-Dec-2019] (2010)
- [32] Wireshark Organization. 2019. Wireshark Go Deep. Available at: availableathttps: //www.wireshark.org/ [Online; accessed 31- Jul- 2019].
- [33] Zhice Yang, Jiansong Zhang, Kun Tan, Qian Zhang, and Yongguang Zhang. 2015. Enabling TDMA for today's wireless LANs. In IEEE Conference on Computer Communications (INFOCOM). 1436–1444.
- [34] Junmei Yao, Jun Xu, Sheng Luo, Lu Wang, Chao Yang, Kaishun Wu, and Wei Lou. 2019. Comprehensive Study on MIMO-related Interference Management in WLANs. IEEE Communications Surveys & Tutorials (2019).
- [35] Yunze Zeng, Ioannis Pefkianakis, Kyu-Han Kim, and Prasant Mohapatra. 2017. MU-MIMO-Aware AP selection for 802.11 ac networks. In Proceedings of the 18th ACM International Symposium on Mobile Ad Hoc Networking and Computing. ACM, 19.
- [36] Xinyu Zhang and Kang G Shin. 2011. Delay-optimal broadcast for multihop wireless networks using self-interference cancellation. *IEEE Transactions on Mobile Computing* 12, 1 (2011), 7–20.
- [37] Xinyu Zhang, Karthikeyan Sundaresan, Mohammad A Amir Khojastepour, Sampath Rangarajan, and Kang G Shin. 2013. NEMOx: Scalable network MIMO for wireless networks. In Proceedings of the 19th annual international conference on Mobile computing & networking. 453–464.
- [38] Anfu Zhou, Teng Wei, Xinyu Zhang, Min Liu, and Zhongcheng Li. 2015. Signpost: Scalable MU-MIMO signaling with zero CSI feedback. In Proc. of the 16th ACM International Symposium on Mobile Ad Hoc Networking and Computing. 327–336.
- [39] Yulong Zou, Jia Zhu, Xianbin Wang, and Lajos Hanzo. 2016. A survey on wireless security: Technical challenges, recent advances, and future trends. Proc. IEEE 104, 9 (2016), 1727–1765.